# Hubbard's parameter influence on $Ba_2GdReO_6$ properties, a promising ferromagnetic double Perovskite oxide for thermoelectric applications

Y. Bouchentouf Idriss[a], B. Bouadjemi[b], M. Matougui[b], M. Houari[b,c,*], T. Lantri[b,c], S. Haid[b,d], and S. Bentata[a,b]

[a] *Laboratory of Quantum Physics of Matter and Mathematical Modelling (LPQ3M), Mustapha Stambouli University of Mascara 29000, Algeria*

[b] *Laboratory of Technology and of Solids Properties, Abdelhamid Ibn Badis University, Mostaganem 27000, Algeria*

[c] *University of Relizane 48000, Algeria*

[d] *Faculty of Sciences and Technology, Tissemsilt University, 38004 Tissemsilt, Algeria.*

[*] *e-mail: houari.mohammed@univ-relizane.dz*

Received 8 January 2023; accepted 28 March 2023

In this paper, an exhaustive investigation was carried out on the compound double Perovskite $Ba_2GdReO_6$ including its structural, electronic, magnetic and thermoelectric properties. This study is based on the density functional theory and more explicitly on the full potential linearized augmented plane wave (FP-LAPW), in the context of different approximations as exchange and correlation potential such as: The generalized gradient approximation (GGA) and its corollary the Becke - Johnson approach modified by Trans-Blaha (TB-mBJ) for a better approximation of the gap, and the GGA + U approach (where $U$ is the Hubbard correction term). After an analysis of the results obtained, it turns out that the double perovskite material $Ba_2GdReO_6$ is a ferromagnetic material and has a half-metallic character, moreover, this compound has an integral magnetic moment of 9 $\mu$B, which is in accordance with the rule of Slater-Pauling. From the study of the thermoelectric properties consisting in plotting curves of different parameters such as: the Seebeck coefficient, electrical conductivity per relaxation time $\sigma/\tau$, the electronic thermal conductivity per relaxation time $ke/\tau$ and the merit factor as a function of temperature, based on the GGA+U approximation, which is most suitable for the study of this compound, it emerges that the double Perovskite $Ba_2GdReO_6$ presents thermoelectric performances in medium to high temperature ranges, in view of the high values of the Seebeck coefficient and those of the electrical conductivity as well as a value close to unity for the merit factor, therefore, this compound can be used for thermoelectric applications in this range of temperatures (medium to high).

*Keywords:* FP-LAPW; half-metallicity; electrical conductivity; ferromagnetic; Seebeck coefficient; thermoelectric applications.

DOI: https://doi.org/10.31349/RevMexFis.69.051006

## 1. Introduction

Owing to their variable and interesting properties, Perovskite and double Perovskite compounds (DPs) have attracted the attention of many scientific researchers for the development of innovative materials. Some of the double perovskites with the formula $A_2BB'O_6$ (A = alkaline earth or rare earth metal; B, B' = transition metals or rare earth) turn out to be half metallic materials, which are metallic in one spin channel while insulating in the other such as $Sr_2FeMoO_6$ [1, 2] and $Sr_2FeReO_6$ [3]. The crystal structure of this ordered double perovskites $A_2BB'O_6$ consists of corner sharing $BO_6$ and $B'O_6$ octahedral, which alternate along three cubic axes, and a large (A) cations occupies the hollow formed by the $BO_6-B'O_6$ octahedral. Very interesting physical properties of these compounds can be attributed to small changes in their chemical composition. Thus, depending on the choice of A, B and B′ cations, a wide variety of electrical and magnetic properties emerge such as metallicity, half metallicity, multiferroicity ferromagnetic (FM), ferrimagnetic (FIM), antiferromagnetic (AFM) and colossal magneto resistance [4–10]. This diversity provides opportunities for a wide range of potential applications such as magnetic refrigerant [11, 12], dielectric resonators, voltage controlled oscillators, filter duplexes in mobile phones and satellite communications that operate in the microwave frequency range (300 MHz to 30 GHz) [14], and magneto-optic devices [13], etc. Information technology needs a rising number of material resources for digital storage and processing, these resources are increasingly made with materials that have specific properties [15]. Among these materials, are oxide compounds perovskite of various crystal formations. Other notable chemical, physical and electrical properties characterize double perovskites due to their flexible chemical composition. Tunnel junctions, X-ray storage phosphor materials and scintillators [16], giant magneto-resistive devices [17,18] and other magnetic devices (CMR) [19] are just some of the numerous technological applications of perovskites, which makes it a lively and rich subject of research involving both chemists and physicists. Double perovskites compounds (DPs) are one of the most studied types of materials due to their $A_2BB'O_6$ stoichiometry. Moreover, they have undeniable advantages, such as the ability of using a large majority of elements in the periodic table [20] and whose manufacture is simple, fast and

profitable. The majority of current research has focused on double perovskites with two oxides (DP) due to (i) a variety of crystal structures, (ii) flexible chemical composition and (iii) the possibility of varying electronic and magnetic properties. Halide double perovskites (HDP) compounds, having $A_2BB'X_6$ structure, where B is monovalent and B' is a trivalent element, also known as elpasolite [21], are potential alternative compounds proposed for technical applications various. Furthermore, promising optoelectronic materials based Cs have been successfully synthesized [22–24], these compounds shows remarkable properties and has been utilized in many applications such as scintillators, catalysts [25], photoelectric absorption layers of solar cells [26, 27] and are characterized by a high absorption coefficient and are therefore suitable for photovoltaic application [28–31]. The study carried out in this article concerns the determination of the structural, electrical, magnetic and thermoelectric properties of the double perovskite material $Ba_2GdReO_6$ using the full potential linearized augmented plane wave (FP-LAPW) method with different approximations such as the generalized gradient approximation (GGA), GGA+U and GGA plus modified Becke-Johnson (GGA+mBJ) methods [32]. For the determination of thermoelectric properties, we have used a semi-classical Boltzmann transport theory and rigid band theory as implemented in BoltzTrap code [33], within the Wien2k program in order to evaluate series thermoelectric parameters such as Seebeck coefficient $S$, electrical conductivity, thermal conductivity and figure of merit $ZT$ for this compound, which could indicate a suitable use of these double perovskite materials in spintronic and thermoelectric applications [34–37]. This paper can be divided in four sections: the calculation method is given in Sec. 2, in Sec. 3, the structural, electronic, magnetic and thermoelectric properties of the compound $Ba_2GdReO_6$ are presented and finally Sec. 4 includes a brief conclusion of this study.

## 2. Computational details

To calculate and evaluate the structural, electronic and transport properties (thermoelectric properties) of the double perovskite compound $Ba_2GdReO_6$, we relied on the method of augmented plane waves linearized at full potential (FP-LAPW) [38–40] such as implemented in the WIEN2K code [41]. In addition, different approximation methods have been considered, such as the generalized gradient approximation (GGA), the generalized gradient approximation with the Becke Johnson modification modified by Trans Blaha (mBJ-GGA) to correctly appreciate the value of the gap, the generalized gradient approximation added to the influence of the Coulomb interaction on site (GGA+U) (where U is the Hubbard correlation term), this with the aim of processing and approximating the exchange-correlation functional of rare earth elements Gd and Re, which are highly correlated, in fact, it is a question of making an adequate correction of the GGA approximation by adding the parameter U to it to correctly describe the electronic correlation of the rare earth elements Gd ($4f^7 5d^1$) and Re ($5d^5$) forming part of the double perovskite $Ba_2GdReO_6$. The GGA+U method requires two parameters, the Hubbard parameter U which gives the strength of the Coulomb repulsion between these orbitals and the Hund parameter J which describes the on-site exchange interaction between these orbitals. In this article, we have modified the U parameter taking the values: 2, 4, 6 and 8 eV to properly assess the electronic, magnetic and transport properties of the compound under study [42, 43]. In the calculations reported here, the radii of the muffin-tin spheres were chosen as 2.20, 1.71, 1.68 and 1.40 a.u. for Ba, Gd, Re and O, respectively. In the interstitial region, plane wave functions are limited to $R_{mt}K_{\max} = 8.0$ where $R_{mt}$ indicates the smallest atomic sphere radius and $K_{\max}$ is the maximum value of the largest $K$ vector in the plane wave expansion. The maximum value for partial waves inside atomic spheres was confined to $L_{\max} = 10$ and the number of special $k$-points in the total Brillouin zone was selected as 1000. Self consistent calculations are considered convergent when the total energy is stable within $10^{-5}$ Ry. The unit cell of double Perovskite $Ba_2GdReO_6$ crystallizes in the cubic structure space group Fm3m (the crystal structure is shown in Fig. 1.

As thermoelectric parameter calculations are sensitive to dense sampling of $k$ points, a high density of $150000$ k-points is used to calculate the thermoelectric properties, the latter are determined using the BoltzTrap code [33, 44] implemented in the Wien2k package and the relaxation time is taken as $0.8 \cdot 10^{-15}$ s as suggested in the BoltzTraP user manual.

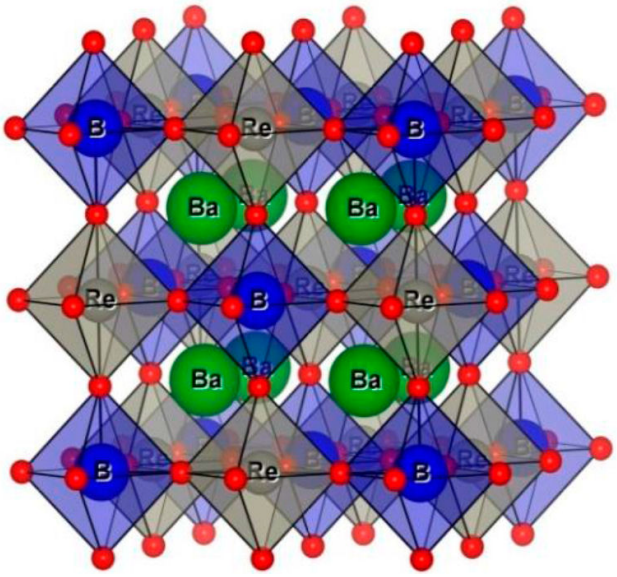


FIGURE 1. Crystal structure of cubic double Perovskite, $Ba_2GdReO_6$.

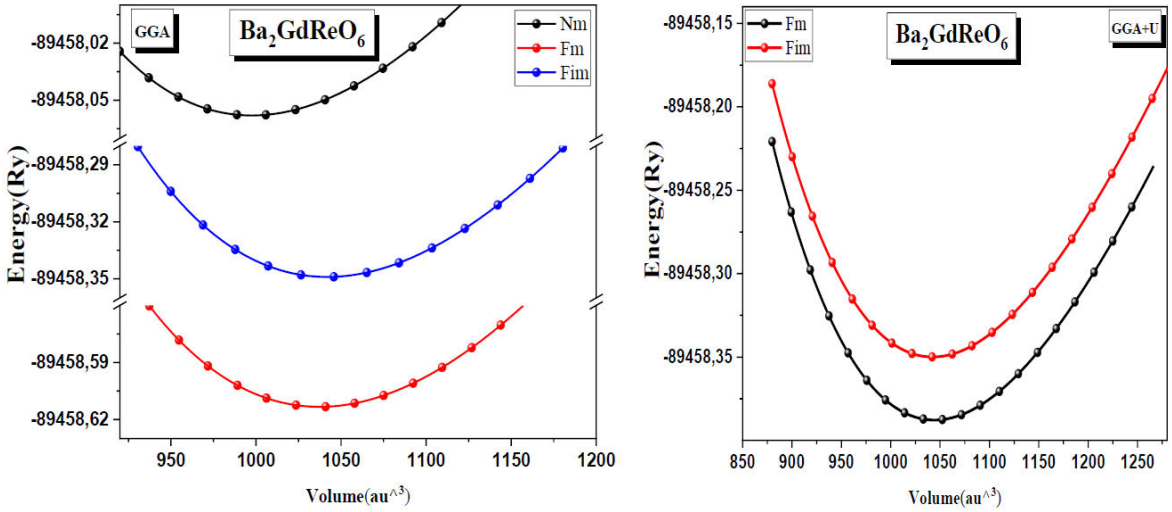


FIGURE 2. Calculated total energy (Ry) as a function of volume for $Ba_2GdReO_6$, using GGA and GGA+U approximations for different magnetic phases.

TABLE I. Calculated equilibrium lattice parameters $a$A, bulk modulus B GPa, its pressure derivative B' and the ground state energy $E$ eV of the cubic double perovskites $Ba_2GdReO_6$, using GGA and GGA+U, in comparison to the available values in the literature.

| Structures parameters | Present work | | other calculation | |
|---|---|---|---|---|
| | GGA | GGA+U | | |
| Lattice parameter $a$ Å | 8.431 | 8.431 | 8.43 [46] | 8.3719 [47] |
| Compressibility module B GPa | 136.33 | 136.94 | / | / |
| Compressibility module derivative B' | 4.096 | 4.706 | / | / |
| Ground state energy $E$ eV | -1217143.229 | -1266646.543 | / | / |

## 3. Results and discussions

### 3.1. Structural properties

The objective of this section is to find the adequate stable state of the compound $Ba_2GdReO_6$. Calculations of the total energies for different volumes were performed using the GGA and GGA+U approximations, following three configurations: the Ferromagnetic (FM), Non-magnetic (NM) and Ferrimagnetic (FiM) configuration. Two configurations were considered when using the GGA+U method: Ferromagnetic (FM) and Ferrimagnetic (FiM). The results obtained by plotting the curves in Fig. 2.

Representing the total energies as a function of the volume, for the two approximations (GGA and GGA+U), reveal that the FM phase has an energy lower than the other phases (NM and FiM), therefore, the double perovskite compound $Ba_2GdReO_6$ in the ferromagnetic state is the most stable in comparison with the other phases. In addition, this fundamental state makes it possible to determine the equilibrium values of the different parameters such as the lattice constant a, bulk modulus B and its pressure derivative B' for this material (Table I), let us recall that the total energies calculated for the double perovskites $Ba_2GdReO_6$ were adjusted by the Birch Murnaghan equation of state [45].

It can be clearly seen that the values of the lattice constants using the GGA and GGA+U approximations are in excellent agreement with those found in the literature [46, 47]. For the bulk modulus B, their experimental and theoretical data are not available; these are therefore predictive studies for future investigations.

### 3.2. Electronics properties

#### *3.2.1. Band structure*

The electronic band structures calculated for the $Ba_2GdReO_6$ material at the equilibrium lattice constant are shown in Fig. 3.

The graphs are structurally similar, but the difference is the gap value given by each approximation. These spectra are calculated for both spins; spin up (↑) and spin down (↓) in the GGA, GGA+U ($U = 4$ eV) and TB-mBJ-GGA approximations. The arrows (↑) and (↓) are the directions of the spins: (↑) for spin-up and (↓) for spin-down. For the $Ba_2GdReO_6$ double perovskite and in the spin-up channel, we observe that the bands overlap at the Fermi level while the states of the conduction band and those of the valence band in the spin-down channel exhibit band gap energy, therefore

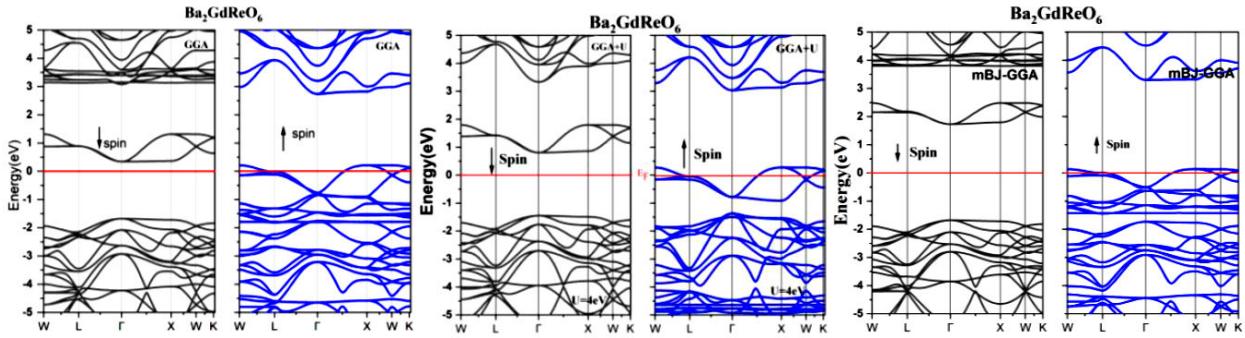


FIGURE 3. Calculated total energy (Ry) as a function of volume for spin-up and spin-down band structures of $Ba_2GdReO_6$ compound using GGA, GGA+U and TB-mBJ approximations.

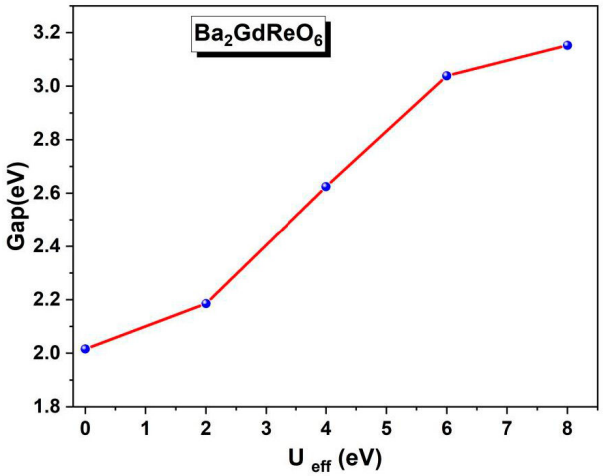


FIGURE 4. Variation of the energy gap as a function of Hubbard parameter $U$ for $Ba_2GdReO_6$.

this compound exhibits a semiconductor behavior in this channel of spin (spin down). From these results, we can deduce that the compound $Ba_2GdReO_6$ has a half-metallic character. Moreover, the energy gap between the valence band maximum and the conduction band minimum is direct in nature, *i.e.* a direct band gap at the point Γ, equal to 2.00 eV, 2.624 eV and 2.670 eV, for the GGA, GGA+U and TB-mBJ-GGA approximations respectively. Using GGA + U (with $U = 2$, 4, 6 and 8 eV) approximation, the band structure dependence with this parameter for $Ba_2GdReO_6$ is shown on Fig. 4.

We notice the increase of band gap with the incensement of Hubbard parameter, with linear increase between $U = 2$ eV to $U = 6$ eV. This figure shows the effect of the parameter $U$ on the band gap values.

### 3.2.2. *Density of states*

In order to delve into the interpretation of the band structure curves, we have plotted the PDOS and the TDOS densities of states for the double Perovskite $Ba_2GdReO_6$, following the approaches using the GGA, the mBJ-GGA and the GGA+U approximations, which are illustrated in Fig. 5. The Fermi

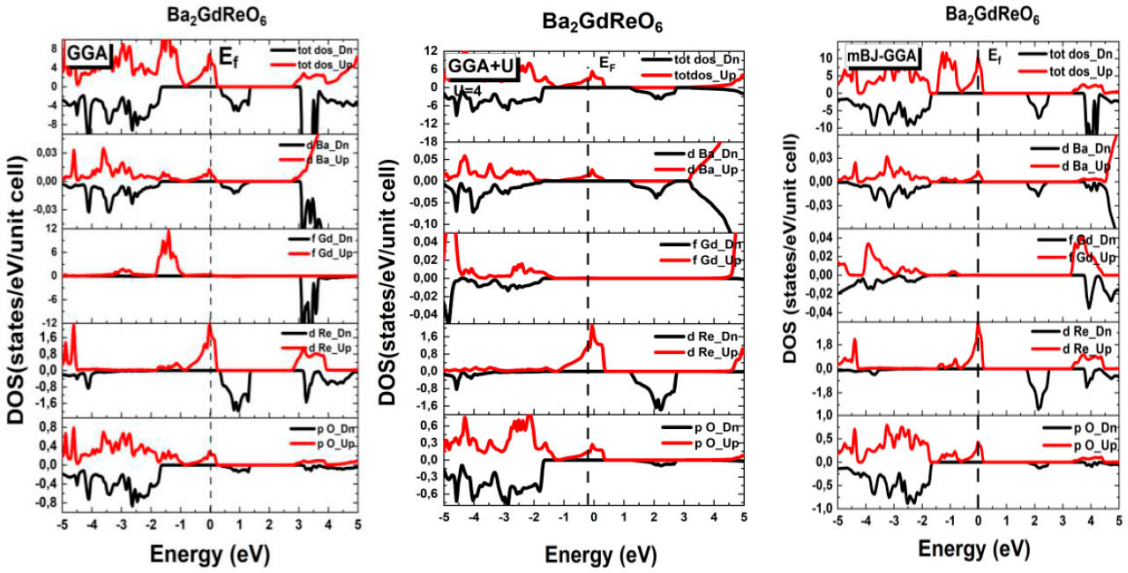


FIGURE 5. Total (TDOS) and partial (PDOS) density of States of $Ba_2GdReO_6$ double perovskite using GGA, GGA+U and Tb-mBJ approximation. Fermi level is set to zero.

level (EF) being represented by a vertical dotted line (0 eV). At first glance, from the calculations carried out according to the three approximations: GGA, GGA+U ($U = 4$ eV), mBJ-GGA and materialized by the curves illustrated in Fig. 5, it is noted that the latter presents a similar aspect as to the shape of the peaks and by the obvious anti symmetric between those of the spin up and those of the spin down with a shift of the peaks different from one approximation to another along with a bursting of the energy bands.The main distinction between the three approximations comes from the fact that the TB-mBJ-GGA approximation estimates a more accurate value of the gap in the spin down channel compared to the other two approximations (GGA and GGA+U).

From the shape of the TDOS curves, it is clear that the $Ba_2GdReO_6$ double perovskite exhibits a half-metallic character; in the spin-up sense (↑) the metallic nature is essentially attributed to strong hybridization of the 5d and 2p orbitals of the Gd and O elements respectively. As it is known, the presence of oxygen atoms around the Gd and Re sites in the compound $Ba_2GdReO_6$ leads to a doubling or even a tripling of these levels, *i.e.* a doubly or triply degenerate state of the Re atom (d, d- *e.g.* and d-t2g); a strong hybridization of these states is at the origin of the gap in the spin down channel. Note that a gap exists between the occupied O (2p) states and the unoccupied Re (d-t2g) states in the spin down channel in the compound $Ba_2GdReO_6$. Furthermore, the valence band maximum is dominated by the O (p) states with a tiny contribution of Re (d-t2g), while the conduction band minimum is dominated by the Re state (d-t2g) as well as the states of Gd atoms. The half-metallic nature of this compound makes it a good opportunity for spintronic applications.

### 3.3. Magnetic properties

The density of states is essential in the determination of the magnetic properties of the double perovskite $Ba_2GdReO_6$ and, in particular, in the proven prediction of the ferromagnetism and the half-metallicity of this material. In order to calculate the magnetic properties of this double perovskite material, we have optimized our calculations for this compound in its ferromagnetic phase as well as the ferrimagnetic and non-magnetic ones. The stable state being in the ferromagnetic phase, this compound is therefore ferromagnetic in nature. For the spin effect, we took the GGA approximation with the inclusion of the Hubbard parameter $U$; the obtained results of the interstitial and total atomic magnetic moments per unit cell in the Bohr magneton $\mu B$ are shown in Table II.

For the compound $Ba_2GdReO_6$, these calculations were performed using the GGA, GGA+U and TB-mBJ-GGA approximations. From the values indicated by this table, it can be noticed that the Re and Gd atoms in the double perovskite $Ba_2GdReO_6$ play an important role to different degrees in the magnetism of the compound studied. This essential contribution obviously comes from the d-d transition in the Re and Gd atoms. Moreover, a minor contribution of other atoms as well as interstitial sites is also involved in the total magnetic

TABLE II. Calculated total $\mu^{\text{Cell}}$, local and interstitial $\mu^{\text{inst}}$ magnetic moments in the units of $\mu B$ for $Ba_2GdReO_6$ double Perovskite.

| | $Ba_2GdReO_6$ | | |
|---|---|---|---|
| | GGA | GGA+U (U=6e V) | mBJ |
| $\mu^{\text{Ba}}$ | 0,0039 | 0,0083 | 0,0037 |
| $\mu^{\text{Gd}}$ | 0,989 | 1,343 | 1,602 |
| $\mu^{\text{Re}}$ | -0.060 | -0.077 | -0.130 |
| $\mu^{\text{O}}$ | 0,021 | 0,005 | 0,013 |
| $\mu^{\text{Cell}}$ | 8,969 | 9,005 | 8.999 |
| $\mu^{\text{inst}}$ | -1 ,3209 | - 0,7759 | - 0,5425 |

moment of the cell; the latter has a positive integral value equal to 9.00 $\mu$B. This integer value of the total magnetic moment confirms the ferromagnetism and the half metallicity of this compound. Note then that the positive values of the magnetic moments of the interstitial sites and of the Gadolinium atoms confirm their alignment parallel to the magnetic moments of Ba. The values of the total magnetic moments according to the GGA, GGA+U and TB-mBJ-GGA methods are 8.969 $\mu$B, 9.005 $\mu$B and 8.999 $\mu$B respectively, these moments come from the Gd ion with a small contribution from the O site. On the other hand, the negative values of the magnetic moments of the Re element with the interstitial sites of the $Ba_2GdReO_6$ material reduce the net magnetic moments of this compound.

### 3.4. Transport properties

Thermoelectricity or conversion of electrical energy from heat is booming with the growing interest in the recovery of waste thermal energy. The conversion of thermal energy into electrical energy is one of these new sources of renewable energy and is of absolute importance because millions of tons of fossil energy are sacrificed every day to obtain electrical energy so essential for our different needs (domestic and industrial). Yet much of this energy is lost to the atmosphere as heat that cannot be efficiently harnessed. However, faced with the growing demand for energy and the desire to use sustainable and renewable sources, this waste heat represents an immense reservoir that can be exploited wisely. Thermoelectric modules, thanks to the Seebeck effect, are able to generate an electric current from a thermal gradient, thus making it possible to exploit the sources of waste heat [48, 49]. In order to describe the thermoelectric behavior of our double perovskite material $Ba_2GdReO_6$, it would be useful to know how a series of fundamental parameters evolve as a function of temperature (or chemical potential) such as electrical conductivity per relaxation time $\sigma/\tau$, the Seebeck (or thermopower) coefficient S, the electronic thermal conductivity per relaxation time $ke/\tau$ and the figure of merit ZT. The variations of these four parameters mentioned previously as a function of the temperature for the double perovskite material $Ba_2GdReO_6$ and according to different approximations,

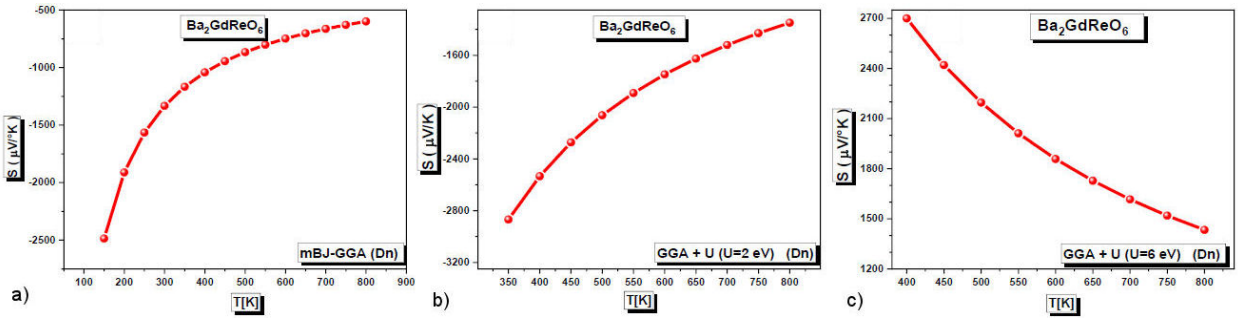


FIGURE 6. Variation of Seebeck coefficient $S$ as a function of temperature for $Ba_2GdReO_6$: a) using mBJ- GGA approximation, b) using GGA+U (U=2eV) approximation and c) using GGA+U ($U = 6$ eV) approximation.

*i.e.* the mBJ-GGA approximation and the GGA+U approximation by varying the Hubbard parameter (2 and 6 eV), are represented by the Figs. 6a), b) and c) for the Seebeck coefficient S following the approximations: mBJ-GGA, GGA+U ($U = 2$ eV) and GGA+U ($U = 6$ eV) respectively; Figures 7a), b) and c) for the electrical conductivity per relaxation time $\sigma/\tau$ following the approximations: mBJ-GGA, GGA+U ($U = 2$ eV) and GGA+U ($U = 6$ eV) respectively; Figures 8a), b) and c) for the electronic thermal conductivity per relaxation time $ke/\tau$ following the approximations: mBJ-GGA, GGA+U ($U = 2$ eV) and GGA+U ($U = 6$ eV) respectively and finally Figs. 9a), b) and c) for the figure of merit (ZT) following the approximations: mBJ-GGA, GGA+U (U=2 eV) and GGA+U ($U = 6$ eV) respectively.

However, good materials suitable for thermoelectric applications must have a high Seebeck coefficient, a high electrical conductivity, a low thermal conductivity and a figure of merit close to unity or greater than unity [50–53], The transport properties of the compound $Ba_2GdReO_6$ were determined using the BoltzTrap code [54] within the Wien2k program, and the approximation for the relaxation time constant $\tau$ as implemented in the BoltzTraP code is taken as $0.8 \times 10^{-14}$ s, as suggested in the BoltzTraP user manual, all these thermoelectric parameters as indicated above are calculated and analysed in the spin down state, and where our material is semi-conductive in nature with gap values of 2 eV, 2.18 eV and 3.03 eV for the approximations: mBJ-GGA, GGA+U ($U = 2$ eV) and GGA+U($U = 6$ eV) respectively. The Seebeck effect is a phenomenon which consists of the appearance of a potential difference at the junction of two materials subjected to a difference (or a gradient) in temperature, this potential difference being generated by the movements of electrons free from the high temperature region to the low temperature region, in materials where the prevailing charge carriers are holes ($p$-type), the Seebeck coefficient has a positive sign, while those dominated by electrons (n-type) have negative Seebeck coefficients. The use of materials with a high Seebeck coefficient is important for a high performance of thermoelectric generators and thermoelectric coolers, *i.e.*, for good thermoelectric predispositions, the material must have a high Seebeck coefficient S. Figure 6 show the variation of the Seebeck coefficient S as a function of temperature for the double perovskite material $Ba_2GdReO_6$, let us note first of all, the high values of the Seebeck coefficient for the three approximations, this is in fact due to strongly degenerated bands in the band structure of this material, according to Fig. 6a) (mBJ-GGA approximation), the Seebeck coefficient increases with the increase in temperature passing from a minimum threshold of $-2485.75$ $\mu$V/K (150 K) up to a maximum threshold of $-599.29$ $\mu$V/K (800 K), similarly, following the GGA+U approximation (Fig. 6b)) with $U = 2$ eV, the Seebeck coefficient increases by a minimum threshold of $-2868.44$ $\mu$V/K (350 K) up to a maximum value of $-1348.26$ $\mu$V/K (800 K) while for the GGA+U approximation [Fig. 6c)] with $U = 6$ eV, the Seebeck coefficient decreases with temperature from a maximum value of 2699.63 $\mu$V/K (400 K) to a minimum value of 1433.63 $\mu$V/K (800 K), in absolute value, the values of the Seebeck coefficients for the three approximations for this material are quite high, which bodes well for thermoelectric applications, in particular with regard to its value at room temperature (330 K) according to the mBJ-GGA approximation and which is: $-1333.01$ $\mu$V/K. Moreover, the values of S obtained turn out to be negative for the two approximations: mBJ-GGA and GGA+U ($U = 2$ eV) for the entire temperature range for the $Ba_2GdReO_6$ material, which implies the presence of N-type charge carriers (electrons) as main carriers, while those obtained through the GGA+U approximation ($U = 6$ eV) are found to be positive for the entire temperature range, which suggests the presence of P-type charge carriers as main carriers. Electrical conductivity defines the ability of a material to allow electrical charges to pass freely. It opposes resistivity, which slows the movement of these charges by resisting it and therefore, electrical conductivity by relaxation time $\sigma/\tau$ conceptualizes the relationship between free charge carriers (holes/electrons) and the current electronic. For suitable applications in the thermoelectric field, the electrical conductivity per relaxation time $\sigma/\tau$ must be sufficiently high because this would imply the reduction of heat losses by Joule effect. The variation of electrical conductivity by relaxation time with temperature for this material is represented by the Figs. 7a), b) and c) according to the above three approximations, the curves are quite similar, one can clearly notice that the electrical conductivity $\sigma/\tau$ is practically lin-

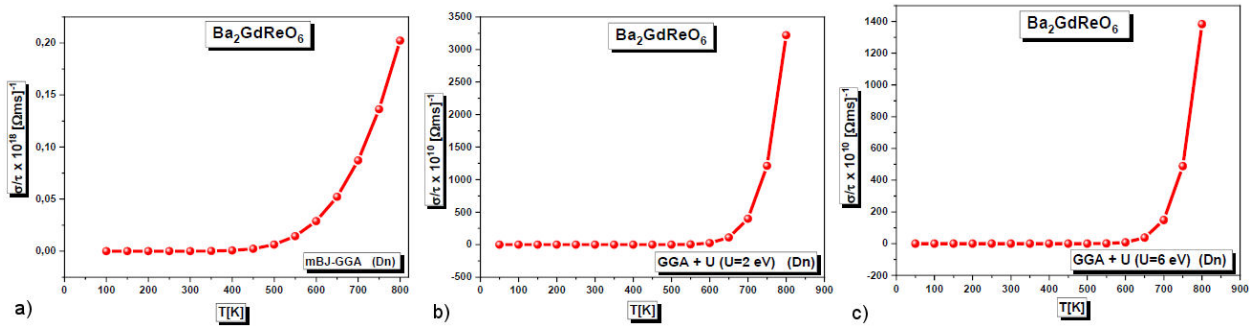


FIGURE 7. Variation of the electrical conductivity per relaxation time ($\sigma/\tau$) as a function of temperature for $Ba_2GdReO_6$: a) using mBJ-GGA approximation, b) using GGA+U ($U = 2$ eV) approximation and c) using GGA+U ($U = 6$ eV) approximation.

ear with the increase in temperature up to a certain threshold (approximately up to $T = 550$ K for the mBJ-GGA approximation and $T = 650$ K for the two other GGA+U approximations with $U = 2$ and 6 eV), it then increases sharply beyond of this temperature threshold, which reflects a semiconductor behavior of the material as predicted by the band structure and the TDOS, the charge carriers (here the electrons) acquire greater mobility as the temperature increases considerably. The maximum values of $\sigma/\tau$ in the $Ba_2GdReO_6$ material are $0.2 \times 10^{18}$ $[\Omega ms]^{-1}$ (800 K), $3.2 \times 10^{13}$ $[\Omega ms]^{-1}$ (800 K) and $1.3 \times 10^{13}$ $[\Omega ms]^{-1}$ (800 K) for the approximations mBJ-GGA, GGA+U ($U = 2$ eV) and GGA+U ($U = 6$ eV) respectively.

We note that the approximation having the smallest gap (in this case the mBJ-GGA approximation having a gap of 2 eV), presents the greatest value of the electrical conductivity, this is due to the fact that, the higher the value of the gap is low, the greater is the concentration of the carriers, which implies a greater mobility of these carriers and consequently a greater electrical conductivity. These results indicate a very high electrical conductivity and consequently a very low resistivity of this material, which implies a transport of electrical charges at very low losses by Joule effect; this is undeniably a major advantage for being a good thermoelectric material. Thermal conductivity is an important parameter that contributes to the optimization of thermoelectric materials. A good thermal conductivity would tend to oppose the establishment of a thermal gradient, the heat would cross the material without encountering resistance, it would therefore be necessary to optimize a thermoelectric material, to reduce the thermal conductivity without degrading the electrical conductivity, given that the thermal conductivity in semiconductor materials comes from the contribution of electrons $K_e$ and phonon such that where and are the electronic part (electrons and holes transporting heat) and the vibration part of the lattice (contribution of phonon) respectively, it is the contribution of the vibrations of the lattice which must be reduced and not the contribution due to the charge carriers (electrons and holes). Figure 8 shows the evolution of the electronic thermal conductivity by relaxation time $k_e/\tau$ as a function of the temperature for the $Ba_2GdReO_6$ material according to the three aforementioned approximations, by these curves, the thermal conductivity for the material studied, increases with the increase of the temperature. It should be noted that the plots of electrical and electronic thermal conductivity have a very similar appearance, in fact, these results are in agreement with the law of Wiedemann-Franz which states a proportionality between these two quantities as follows [55]:

$$K = \sigma L T, \tag{1}$$

where $L$ is the Lorenz number; $\sigma$ represents electrical conductivity while $T$ is absolute temperature. The electronic thermal conductivity value is approximately $9.35 \times 10^{-5}$ [W/mKs] at room temperature ($T = 300$ K) for the mBJ-GGA approximation. The qualities of a thermoelectric material are measured by a dimensionless number, called figure of merit ZT given by the relation:

$$ZT = \frac{S^2 T}{\sigma . K}, \tag{2}$$

where $T$ the absolute temperature, $S$ the Seebeck coefficient, $\sigma$ the electrical conductivity and $K$ the thermal conductivity. In order to optimize the transport properties of a material, the figure of merit $ZT$ must be as high as possible (close to or greater than unity), which implies that the Seebeck coefficient $S$ and the electrical conductivity must be as large as possible while the thermal conductivity must be minimized without affecting the electronic transport of charges. Figure 9 shows the plot of the merit factor $ZT$ as a function of the temperature $T$, by the evolution of these curves, the merit factor $ZT$ decreases with the temperature, going from a maximum value of 0.99 (150 K) to a minimum value of 0.96 (800 K) for the mBJ-GGA approximation, with respect to the approximation GGA+U ($U = 2$ eV), it goes from 0.99 (350 K) up to the value of 0.98 (800 K) while for the approximation GGA+U ($U = 6$ eV), it decreases from 0.997 (400 K) to 0.993 (800 K). However, this decrease does not imply a significant degradation of the merit factor $ZT$, because it keeps very suitable values (close to unit) and therefore very interesting for thermoelectric applications. At room temperature (300 K) the value of figure of merit $ZT$ is 0.991 for the mBJ-GGA approximation. Due to the fairly substantial value of the figure of merit ZT, the double perovskite material $Ba_2GdReO_6$ has excellent predisposition in the thermoelectric field.

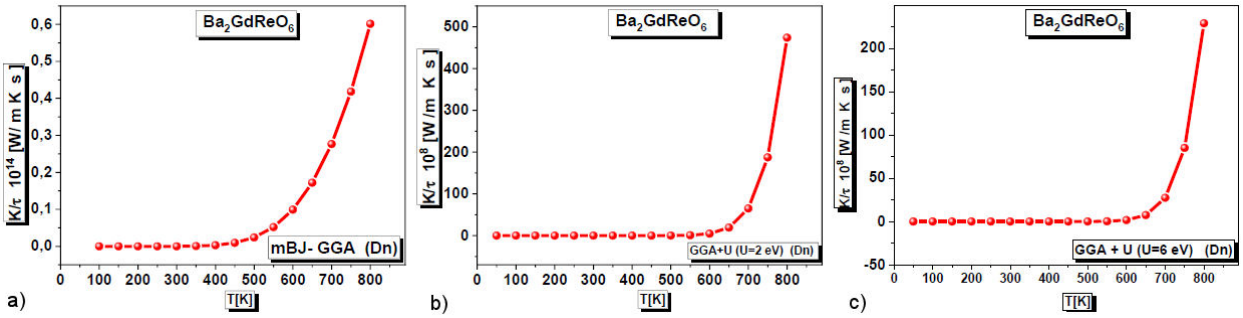


FIGURE 8. Variation of the electronic thermal conductivity per relaxation time ($ke/\tau$) as a function of temperature for $Ba_2GdReO_6$: a) using mBJ- GGA approximation, b) using GGA+U ($U = 2$ eV) approximation and c) using GGA+U ($U = 6$ eV) approximation.

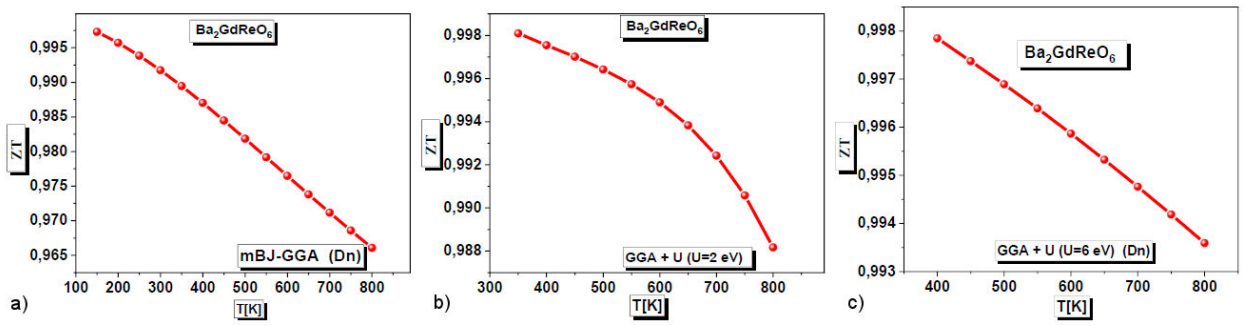


FIGURE 9. Variation of the figure of merit (ZT) as a function of temperature for $Ba_2GdReO_6$: a) using mBJ- GGA approximation, b) using GGA+U ($U = 2$ eV) approximation and c) using GGA+U ($U = 6$ eV) approximation.

By introducing Hubbard's parameter in the GGA approximation ($U = 2$ and 6 eV), apart from the representative curves of electrical and thermal conductivity by relaxation time, being all similar for the three approximations considered (mBJ-GGA, GGA+U ($U = 2$ eV) and GGA+U ($U = 6$ eV)), the notable differences come from the shape of the curves of the Seebeck coefficient and the merit factor, with regard to the Seebeck coefficient, it was affected compared to the mBJ-GGA approximation, because of the positive values acquired for $U = 6$ eV. Moreover, the Seebeck coefficient and the merit factor under the GGA+U approximation ($U = 2$ eV and 6 eV), are observable and quantifiable from a certain temperature threshold, in this case $T = 350$ K for the two values of the parameter of Hubbard, which makes this material thermoelectrically efficient for mid-range and high temperatures, unlike the mBJ-GGA approximation, and where this material is thermoelectrically efficient for the entire temperature range, by favoring the GGA+U approach, which in my opinion is the most suitable for the study of this material. As no experimental study has been made on this material, it would be highly beneficial to do so to confirm these results.

## 4. Conclusion

In summary, based on the Full Potential Linearized Augmented Plane Wave (FP-LAPW) method, and advocating as exchange and correlation potentials the following three approaches: the Generalized Gradient Approximation (GGA), the generalized gradient approximation with the Becke-Johnson modification modified by Trans-Blaha (TB-mBJ-GGA and the generalized gradient approximation with Hubbard parameter U (GGA+U), we performed extensive research to calculate and evaluate the structural, electronic, magnetic and thermoelectric properties of the rare-earth-based double perovskite compound $Ba_2GdReO_6$. From the results obtained, we can deduce that this material is stable in its ferromagnetic phase, moreover, by the analysis of the electronic properties, it turns out that this compound is half -metallic in nature: metallic nature in spin up channel and semiconductor one in spin down channel with a direct gap equal to 2.00 eV, 2.624 eV and 2.670 eV for the GGA, GGA+U and TB-mBJ-GGA approximations respectively, and therefore presents an interest evident for spintronic applications. Moreover, this double perovskite compound, due to the substantial value of the merit factor (nearing unity for the three approximations) shows very interesting thermoelectric predispositions in the minority spin or spin down channel. Note this singularity in the approximation GGA+U ($U = 2$ and 6 eV), and where the Seebeck coefficient and the merit factor are appreciable and quantifiable from a certain temperature threshold, in this case $T = 350$ K, therefore, this material is an excellent thermoelectric $TE$ material for medium and high temperatures. Our theoretical predictions of the structural, electronic and thermoelectric properties of the double perovskite $Ba_2GdReO_6$ are awaiting confirmation and experimental verification.

1. D. Sarma, A new class of magnetic materials: $Sr_2FeReO_6$ and related compounds. *Current Opinion in Solid State and Materials Science* **5** ( 2001) 261, https://doi.org/10.1016/S1359-0286(01)00014-6
2. K. I. Kobayashi *et al.*, Room-temperature magnetoresistance in an oxide material with an ordered double-perovskite structure. *Nature,* **395** (1998) 677, https://doi.org/10.1038/27167
3. K. I. Kobayashi *et al.*, Intergrain tunneling magnetoresistance in polycrystals of the ordered double perovskite $Sr_2FeReO_6$, *Phys. Rev. B* **59** (1999) 11159, https://doi.org/10.1103/PhysRevB.59.11159
4. G. Vaitheeswaran, V. Kanchana, and A. Delin, Pseudo-half-metallicity in the double perovskite $Sr_2FeReO_6$ from density-functional calculations. *Applied Physics Letters,* **86** (2005) 032513, https://doi.org/10.1063/1.1855418
5. W. E. Pickett, Spin-density-functional-based search for half-metallic antiferromagnets. *Physical review B* **57** (1998) 10613, https://doi.org/10.1103/PhysRevB.57.10613
6. E. Carvalho, E. Diniz, and C. Paschoal, Behavior of the elastic and mechanical properties of $Ba_2BiTaO_6$ compound under pressure changes. *Computational materials science*. **40** (2007) 417, https://doi.org/10.1016/j.commatsci.2007.01.020
7. S. Kumar, *et al*, Theoretical prediction of multiferroicity in double perovskite Y 2 NiMnO 6. *Physical Review B* **82** (2010) 134429, https://doi.org/10.1103/PhysRevB.82.134429
8. M. Azuma *et al.*, Designed ferromagnetic, ferroelectric Bi2NiMnO6. *Journal of the American Chemical Society* **127** (2005) 8889, https://doi.org/10.1021/ja0512576
9. C. Meneghini *et al.*, Nature of "disorder" in the ordered double perovskite Sr 2 FeMoO 6. *Physical Review Letters* **103** (2009) 046403, https://doi.org/10.1103/PhysRevLett.103.046403
10. S. Lv *et al.*, Magnetic and electronic structures of Ba2MnMoO6 from first-principles calculations, *Computational materials science* **49** (2010)266, https://doi.org/10.31349/RevMexFis.64.326
11. G. Sharma *et al.*, Magnetic entropy change and critical exponents in double perovskite Y2NiMnO6. *Journal of magnetism and magnetic materials* **368** (2014) 318, https://doi.org/10.1016/j.jmmm.2014.05.035
12. V. Franco *et al.*, The magnetocaloric effect and magnetic refrigeration near room temperature: materials and models. *Annual Review of Materials Research* **42** (2012) 305, https://doi.org/10.1146/annurev-matsci-062910-100356
13. I. Gorodea, M. Goanta, and M. Toma, Impact of A cation size of double perovskite A2AlTaO6 (A= Ca, Sr, Ba) on dielectric and catalytic properties. *Journal of Alloys and Compounds* **632** (2015) 805, https://doi.org/10.1016/j.jallcom.2015.01.310
14. H. Das, M. De Raychaudhury, and T. Saha-Dasgupta, Moderate to large magneto-optical signals in high T c double perovskites. *Applied Physics Letters* **92** (2008) 201912, https://doi.org/10.1063/1.2936304
15. S. Haid *et al.*, Optical properties of half-metallic ferrimagnetic double perovskite Sr2CaOsO6 compound. *Solid State Communications* **322** (2020) 114052, https://doi.org/10.1016/j.ssc.2020.114052
16. M. Houari *et al.*, Structural, electronic and optical properties of cubic fluoroelpasolite Cs2NaYF6 by density functional theory. *Chinese Journal of Physics* **56** (2018) 1756, https://doi.org/10.1016/j.cjph.2018.05.004
17. A. Souidi *et al.*, First principle study of spintronic properties for double perovskites Ba2XMoO6 with X= V, Cr and Mn. *Materials Science in Semiconductor Processing* **43** (2016) 196, https://doi.org/10.1016/j.mssp.2015.12.017
18. B. Djeltiv *et al.*, Elastic, magnetic and electronic properties of ferrimagnetic double perovskite Sr 2 MnWO 6 using GGA+ U and mBJ-GGA. *Applied Physics A* **124** (2018) 1, https://doi.org/10.1007/s00339-018-2051-1
19. S. Haid *et al.*, Magnetic, Optoelectronic, and Thermodynamic Properties of Sr2Cr XO6 (X= La and Y): Half-Metallic and Ferromagnetic Behavior. *Journal of Superconductivity and Novel Magnetism* **31** (2018) 3965, https://doi.org/10.1007/s10948-018-4643-6
20. R. W. McKinney, Search for new thermoelectric materials with low Lorenz number, *Journal of Materials Chemistry A* **5** (2017) 17302-17311 https://doi.org/10.1039/C7TA04332E
21. K. M. Nicholson, S. G. Kang, and D. S. Sholl, First principles methods for elpasolite halide crystal structure prediction at finite temperatures. *Journal of alloys and compounds* **577** (2013) 463, https://doi.org/10.1016/j.jallcom.2013.06.032
22. M. Falin *et al.*, Optical spectroscopy of Yb3+ in the Cs2NaYF6 single crystal. *Journal of luminescence* **128** (2008) 1103, https://doi.org/10.1016/j.jlumin.2007.10.004
23. S. Ananthakumar, J.R. Kumar, and S.M. Babu, Cesium lead halide (CsPbX 3, X= Cl, Br, I) perovskite quantum dots-synthesis, properties, and applications: a review of their present status. *Journal of Photonics for Energy* **6** (2016) 042001, https://doi.org/10.1117/1.JPE.6.042001
24. M. Roknuzzaman *et al.*, Electronic and optical properties of lead-free hybrid double perovskites for photovoltaic and optoelectronic applications. *Scientific reports* **9** (2019) 1, https://doi.org/10.1038/s41598-018-37132-2
25. X. Xu, Y. Zhong, and Z. Shao, Double perovskites in catalysis, electrocatalysis, and photo (electro) catalysis. *Trends in Chemistry* **1** (2019) 410, https://doi.org/10.1016/j.trechm.2019.05.006
26. X. Du *et al.*, Insights on electronic structures, elastic features and optical properties of mixed-valence double perovskites Cs2Au2X6 (X= F, Cl, Br, I). *Physics Letters A* **384** (2020) 126169, https://doi.org/10.1016/j.physleta.2019.126169

27. E. Haque, and M. A. Hossain, Electronic, phonon transport and thermoelectric properties of Cs2InAgCl6 from first-principles study. *Computational Condensed Matter* **19** (2019) e00374, https://doi.org/10.1016/j.cocom.2019.e00374

28. B. Bouadjemi *et al.,* Ab-initio investigation of optoelectronic properties for elpasolite Cs2NaVCl6 using GGA+ U approach: band gap engineering. *Computational Condensed Matter* **26** (2021) e00531, https://doi.org/10.1016/j.cocom.2020.e00531

29. G. Liu *et al.,* Ultraviolet-Protective Transparent Photovoltaics Based on Lead-Free Double Perovskites. *Solar RRL* **4** (2020) 2000056, https://doi.org/10.1002/solr.202000056

30. N. Shahed *et al.,* Effect of oxygen deficiency on optical and magnetic properties of Ba2MMoO6 (M= Cr, Mn, Fe): A first-principles study. *Computational Condensed Matter* **23** (2020) e00464, https://doi.org/10.1016/j.cocom.2020.e00464

31. M. Matougui *et al.,* A DFT study of new full Heusler compound Li2MgC Insights into the Structural, electronic and thermoelectric properties: A High Efficiency performance thermoelectric material. *Chemical Physics Letters* (2023) 140352, https://doi.org/10.1016/j.cplett.2023.140352

32. F. Tran, and P. Blaha, Accurate band gaps of semiconductors and insulators with a semilocal exchange-correlation potential. *Physical review letters* **102** (2009) 226401, https://doi.org/10.1103/PhysRevLett.102.22640

33. G. K. Madsen, and D.J. Singh, BoltzTraP. A code for calculating band-structure dependent quantities. *Computer Physics Communications* **175** (2006) 67, https://doi.org/10.1016/j.cpc.2006.03.007

34. M. Matougui *et al.,* Electronic structure, mechanical and thermoelectric properties of the full Heusler Ba 2 AgZ (Z= Bi, Sb) alloys: insights from DFT study. *Indian Journal of Physics* (2021) 1, https://doi.org/10.1007/s12648-020-01943-9

35. M. Houari *et al.,* Electronic Structure and Thermoelectric Properties of Semiconductors K2GeSiX6 (X=F, Cl, Br and I) Compounds: *Ab-Initio Investigation. SPIN* **11** (2021) 2150009, https://doi.org/10.1142/S2010324721500090

36. R. Bentata *et al.,* New p-type sp-based half-Heusler compounds LiBaX (X= Si, Ge) for spintronics and thermoelectricity via ab-initio calculations. *Journal of Computational Electronics* **20** (2021) 1072, https://doi.org/10.1007/s10825-021-01702-x

37. S. Haid *et al.,* Predictive study of the rare earth double perovskite Oxide Ba2ErReO6 and the influence of the hubbard parameter U on its half-metallicity. *Journal of Superconductivity and Novel Magnetism* **34** (2021) 2893, https://doi.org/10.1007/s10948-021-06011-9

38. O. K. Andersen, and O. Jepsen, Explicit first-principles tight-binding theory. *Physical Review Letters*, **53** (1984) 2571, https://doi.org/10.1103/PhysRevLett.53.2571

39. K. Mun Wong *et al.,* First-principles investigation of the size-dependent structural stability and electronic properties of O-vacancies at the ZnO polar and non-polar surfaces. *Journal of Applied Physics* **113** (2013) 014304, https://doi.org/10.1063/1.4772647

40. K. Mun Wong *et al.,* Spatial distribution of neutral oxygen vacancies on ZnO nanowire surfaces: an investigation combining confocal microscopy and first principles calculations. *Journal of Applied Physics* **114** (2013) 034901, https://doi.org/10.1063/1.4813517

41. P. Blaha *et al.,* wien2k. *An augmented plane wave+ local orbitals program for calculating crystal properties* **60** (2001) 1, https://doi.org/10.1016/S0927-0256(03)00112-5

42. J. P. Perdew, K. Burke, and M. Ernzerhof, Generalized gradient approximation made simple. *Physical review letters* **77** (1996) 3865, https://doi.org/10.1103/PhysRevLett.77.3865

43. T. Rezkallah *et al.,* Investigation of the electronic and magnetic properties of Mn doped ZnO using the FP-LAPW method. *Chinese journal of physics* **55** (2017) 1432, https://doi.org/10.1016/j.cjph.2017.02.021

44. A. Bouadi *et al.,* A new semiconducting full Heusler Li2BeX (X= Si, Ge and Sn): first-principles phonon and Boltzmann calculations. *Physica Scripta* **97** (2022) 105710, https://doi.org/10.1088/1402-4896/ac925f

45. F. D. Murnaghan, The compressibility of media under extreme pressures. *Proceedings of the National Academy of Sciences* **30** (1944) 244, https://doi.org/10.1073/pnas.30.9.24

46. S. Dimitrovska, S. Aleksovska and I. Kuzmanovski, Prediction of the unit cell edge length of cubic A2 BBO6 perovskites by multiple linear regression and artificial neural networks. *Central European Journal of Chemistry* **3** (2005) 198, https://doi.org/10.2478/BF02476250

47. R. Ullah *et al*., Effect of cation exchange on structural, electronic, magnetic and transport properties of Ba2MReO6 (M= In, Gd). *Journal of Magnetism and Magnetic Materials* **546** (2022) 168816, https://doi.org/10.1016/j.jmmm.2021.168816

48. S. A. Sofi,and D. C. Gupta, Robustness in ferromagnetic phase stability, half-metallic behavior and transport properties of cobalt-based full-Heuslers compounds: A first principles approach. *International Journal of Quantum Chemistry* **121** (2021) e26538, https://doi.org/10.1002/qua.26538

49. P. K. Kamlesh *et al*., Investigation of inherent properties of XScZ (X= Li, Na, K; Z= C, Si, Ge) half-Heusler compounds: appropriate for photovoltaic and thermoelectric applications. *Physica B: Condensed Matter* **615** (2021) 412536, https://doi.org/10.1016/j.physb.2020.412536

50. S. Haid *et al*., Thermoelectric, structural, optoelectronic and magnetic properties of double perovskite Sr2CrTaO6: first principle study. *Materials Science and Engineering: B* **245** (2019) 68, https://doi.org/10.1016/j.mseb.2019.05.013

51. B. Bouadjemi *et al*., High spin polarization and thermoelectric efficiency of half-metallic ferromagnetic CrYSn (Y= Ca, Sr) of half-heusler compounds. *in Spin* (2020) 2050010, https://doi.org/10.1142/S2010324720500101

52. M. Matougui *et al*., Rattling Heusler semiconductors' thermoelectric properties: First-principles prediction. *Chinese journal of physics* https://doi.org/10.1016/j.cjph.2018.11.015

53. M. Houari *et al*., Semi 3 (A = K, Rb and Cs, X = F, Cl and Br),first principles calculations, *Indian Journal of Physics* **94** (2020) 455, https://doi.org/10.1007/s12648-019-01480-0

54. A. Roy *et al*., Single crystalline ultrathin gold nanowires: *Promising nanoscale interconnects. AIP Advances* **3** (2013) 032131, https://doi.org/10.1063/1.4796188.

55. A. Bejan,and A. D. Kraus, Heat transfer handbook1. John Wiley Sons (2013).